
ENHANCING FACIAL CLASSIFICATION AND RECOGNITION USING 3D FACIAL MODELS AND DEEP LEARNING

Houting Li*

Department of Mathematics
The Chinese University of Hong Kong
Hong Kong
hooting@link.cuhk.edu.hk

Mengxuan Dong*

Department of Mathematics
The Chinese University of Hong Kong
Hong Kong
dongmengxuan@link.cuhk.edu.hk

Lok Ming Lui

Department of Mathematics
The Chinese University of Hong Kong
Hong Kong
lmlui@math.cuhk.edu.hk

December 11, 2023

ABSTRACT

Accurate analysis and classification of facial attributes are essential in various applications, from human-computer interaction to security systems. In this work, a novel approach to enhance facial classification and recognition tasks through the integration of 3D facial models with deep learning methods was proposed. We extract the most useful information for various tasks using the 3D Facial Model, leading to improved classification accuracy. Combining 3D facial insights with ResNet architecture, our approach achieves notable results: 100% individual classification, 95.4% gender classification, and 83.5% expression classification accuracy. This method holds promise for advancing facial analysis and recognition research.

*These authors contributed equally to this work.

1 Introduction

Accurate classification and recognition, encompassing tasks like individual identification, emotion recognition, and gender classification, is of significant importance within the realm of computer vision applications. These tasks find utility across a wide spectrum, ranging from enhancing human-computer interaction to strengthen security systems.

In the context of image classification, Convolutional Neural Networks (CNNs) stand as the cornerstone of deep learning algorithms. Well-established models such as FaceNet[1] and ResNets[2] have demonstrated their capacity and efficacy in image classification tasks. However, it's important to note that the effectiveness of these models in identifying crucial features can vary across different tasks. Our work focuses on a method to extract the most informative features before training. The resulting models can then leverage this information during both the training and validation processes, thereby directly enhancing their performance.

2 Previous Work

Advancements in facial classification and recognition have been significantly influenced by deep learning approaches. Yi Sun, Xiaogang Wang, and Xiaoou Tang, in their work DeepID[3] introduced Deep hidden IDentity features. These features, derived from deep convolutional networks, are learned through multi-class face identification tasks and can generalize to tasks like verification and identities unseen in the training set. With the capability to recognize around 10,000 face identities, these features achieve high verification accuracy, even with weakly aligned faces.

Another notable contribution is from Y Taigman, M Yang, MA Ranzato, and L Wolf in their study Deepface[4] They revisited the alignment and representation stages of face recognition by employing explicit 3D face modeling and a nine-layer deep neural network. This approach, trained on a large dataset of four million facial images, significantly reduced the error in face verification, approaching near-human-level performance. This is a cornerstone work to incorporate 3D information in human facial classifications.

Following these groundbreaking studies, other research has focused on more dataset-specific advancements. Eng et al.[5] used histogram of oriented gradients (HOG) and support vector machines (SVM) for facial expression recognition on the KDEF dataset, achieving an accuracy of 80.95%. In gender classification, Thomaz and Giraldi[6] implemented a novel ranking method for principal component analysis (PCA) on the FEI database, achieving around 97% accuracy.

3 Contribution

Our intuition started from a 3D Face Reconstruction based classification model[7]. In their study, they utilized 3D face reconstruction by 3D Morphable Model (3DMM)[8] from images. After face reconstruction, they computed geometry feature in the 3D face mesh for disease diagnosis. But computations and reconstructions may causes severe information loss - Can we use informative parameters to avoid the loss caused by complicated computational process? In this paper, we propose a novel approach to address various classification tasks by integrating the power of the 3DMM with the versatility of ResNet architecture. The 3DMM serves as a pivotal tool for extracting shape and expression information, while ResNet operates as our classification model. Beside, an approach utilizing information from images in multiple angles increase accuracy in 3DMM[9]. Notably, we find that the parameters derived from the 3D Facial Model outperform the use of original images in facial classification tasks. Our approach systematically extracts the most salient information suited for distinct classification endeavors, thereby leading to improved accuracy levels. Empirical results underscore the potency of our method, achieving remarkable milestones such as 100% accuracy in individual classification, 95.4% accuracy in gender classification, and 83.5% accuracy in expression classification.

4 Datasets

4.1 KDEF Dataset

The Karolinska Directed Emotional Faces (KDEF) dataset[10], developed by Lundqvist, Flykt, and Öhman in 1998, is a comprehensive collection of 4900 images, showcasing 70 individuals (35 females and 35 males, aged 20-30 years) displaying seven different emotional expressions: afraid, angry, disgust, happy, neutral, sad, and surprise. Each expression is captured from five angles, providing a multi-dimensional view of human emotions.

Subjects were selected based on specific criteria, such as the absence of facial hair, eyeglasses, and noticeable makeup. They rehearsed emotions to ensure natural and clear expressions. The photographs were taken using a Pentax LX camera with a 135 mm lens and Kodak 320 T film. The lighting was designed to uniformly illuminate the face without harsh shadows. Digitization involved a Macintosh 8500/120 with a Polaroid Sprintsan 35, using Adobe Photoshop 4 for processing. Images were scanned in RGB color at 625 dpi and cropped to 562 x 762 pixels. Each JPEG image is coded for easy identification of session, gender, identity, expression, and angle.



Figure 1: Examples from KDEF Dataset (F04HA & F04NE)

4.2 FEI Face Database

The FEI Face Database[11] is a Brazilian face database that contains a set of face images taken between June 2005 and March 2006 at the Artificial Intelligence Laboratory of FEI in São Bernardo do Campo, São Paulo, Brazil. There are 14 images for each of 200 individuals, a total of 2800 images. All images are colourful and taken against a white homogenous background in an upright frontal position with profile rotation of up to about 180 degrees. Scale might vary about 10%. The original size of each image is 640×480 pixels. All faces are mainly represented by students and staff at FEI, between 19 and 40 years old with distinct appearance, hairstyle, and adorns. The number of male and female subjects are exactly the same and equal to 100.

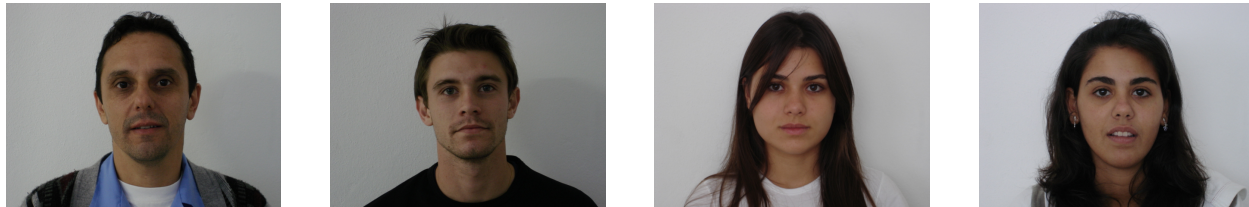


Figure 2: Examples from FEI Face Database

5 Method

The parameters α and β used for classification can be obtained in 3D Facial Model Reconstruction. In 5.1, we adopt R-Net and C-Net from multiple images[9] to extract α and β , where α mainly influence shape and β influence expression. R-Net will be used to extract parameters that influence 3D Facial Reconstruction, while C-Net is to learn how to utilize information from different angles. Then use α and β to train ResNet-34 respectively for different classification purpose. The framework of the flow is presented in the following chart.

(a) Framework for individual / gender classification

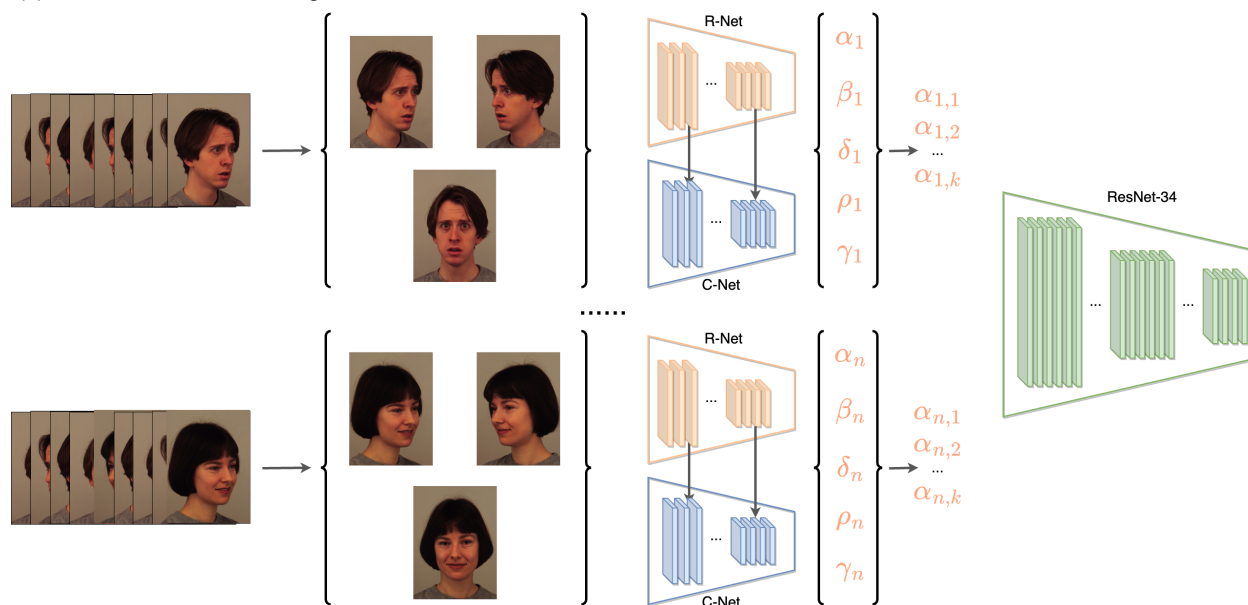


Figure 3: Framework for Individual/Gender Classification using Convolutional Neural Networks. The process starts with multiple angle images of individuals, which are fed into the R-Net to extract feature vectors. C-Net is used to make an accurate reconstruction from multiple images. After generated α , it will be used to train ResNet-34 for classification

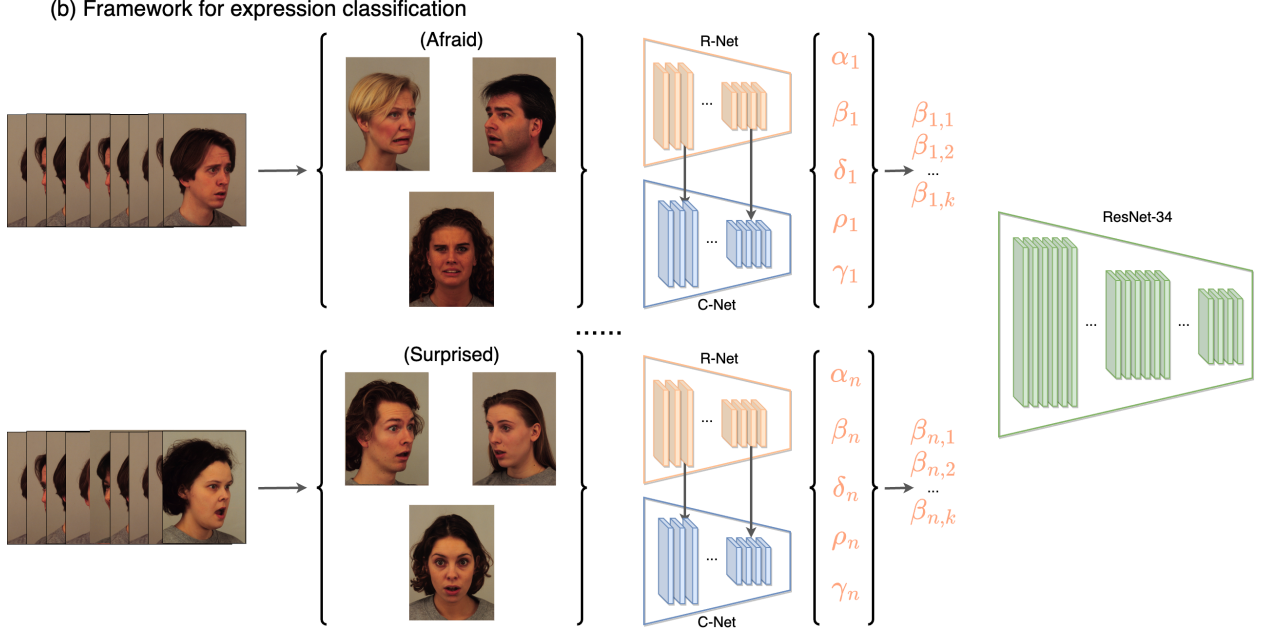


Figure 4: Framework for Expression Classification using Convolutional Neural Networks. The process is similar as previous figure.

5.1 3D Facial Model Reconstruction

The first step is to obtain a 3DMM parameter α and β for network training and classification purpose. α is the only parameter that influences face shape in Basel Face Model, and β is the parameter that influences expressions on faces. This 3D Facial Model can reconstruct a 3D representation of the face shape from a 2D images. The model uses a modified ResNet-34 (R-Net) to regress coefficients of a 3DMM face model, illumination model and camera model.

For 3D Face Model, With a 3DMM, the face shape \mathbf{S} and the texture \mathbf{T} can be represented as: For 3D Face Model, With a 3DMM, the face shape \mathbf{S} and the texture \mathbf{T} can be represented as:

$$\mathbf{S} = \mathbf{S}(\alpha, \beta) = \bar{\mathbf{S}} + \mathbf{B}_{id}\alpha + \mathbf{B}_{exp}\beta$$

$$\mathbf{T} = \mathbf{T}(\delta) = \bar{\mathbf{T}} + \mathbf{B}_t\delta$$

where $\bar{\mathbf{S}}$ and $\bar{\mathbf{T}}$ are the average face shape and texture; \mathbf{B}_{id} , \mathbf{B}_{exp} , and \mathbf{B}_t are the PCA bases of identity, expression, and texture respectively; α , β , and δ are the corresponding coefficient vectors for generating a 3D face. The Basel Face Model [12] is used for $\bar{\mathbf{S}}$, \mathbf{B}_{id} , $\bar{\mathbf{T}}$, and \mathbf{B}_t , and the expression bases \mathbf{B}_{exp} in [13] are used. A subset of the bases is selected, resulting in $\alpha \in \mathbb{R}^{80}$, $\beta \in \mathbb{R}^{64}$, and $\delta \in \mathbb{R}^{80}$.

For the Illumination Model, the scene illumination is approximated with Spherical Harmonics (SH)[14, 15]. The radiosity of a vertex s_i with surface normal n_i and skin texture t_i can then be computed as $C(n_i, t_i | \gamma) = t_i \cdot \sum_{b=1}^{B^2} \gamma_b \Phi_b(n_i)$, where $\Phi_b : \mathbb{R}^3 \rightarrow \mathbb{R}$ are SH basis functions and γ_b are the corresponding SH coefficients. We choose $B = 3$ bands and assume monochromatic lights, such that $\gamma \in \mathbb{R}^9$.

For the Camera Model, we use the perspective camera model with an empirically-selected focal length for the 3D-2D projection geometry. The 3D face pose p is represented by rotation $R \in \text{SO}(3)$ and translation $t \in \mathbb{R}^3$.

In summary, the unknowns to be predicted can be represented by a vector $\mathbf{x} = (\alpha, \beta, \delta, \gamma, p) \in \mathbb{R}^{239}$. The loss functions are shown in the following section.

5.1.1 Hybrid-level Weak-supervision for Single-Image Reconstruction

Given a training RGB image I , we use R-Net to regress a coefficient vector \mathbf{x} , with which a reconstructed image I' can be analytically generated with some simple, differentiable math derivations.

The robust photometric loss is defined as:

$$L_{\text{photo}}(\mathbf{x}) = \frac{\sum_{i \in M} A_i \cdot \|I_i - I'_i(\mathbf{x})\|_2}{\sum_{i \in M} A_i}$$

where i denotes the pixel index, M is the reprojected face region, and A is a skin color-based attention mask for the training image, described as follows.

For skin attention, to gain robustness to occlusions and other challenging appearance variations such as beard and heavy makeup, a skin-color probability P_i is computed for each pixel. A naive Bayes classifier with Gaussian Mixture Models is trained on a skin image dataset from [16]. For each pixel i , we set $A_i = \begin{cases} 1, & \text{if } P_i > 0.5, \\ P_i, & \text{otherwise.} \end{cases}$

The 3D face alignment method in [17] is used to detect 68 landmarks $\{q_n\}$ of the training images. During training, the 3D landmark vertices of the reconstructed shape are projected onto the image, obtaining $\{q'_n\}$, and the loss is computed as:

$$L_{\text{lan}}(\mathbf{x}) = \frac{1}{N} \sum_{n=1}^N \omega_n \|q_n - q'_n(\mathbf{x})\|^2$$

where ω_n is the landmark weight.

Using low-level information alone can lead to local minimum. To tackle this issue, a perception-level loss is introduced. The deep features of the images are extracted, and the loss is computed as follows:

$$L_{\text{per}}(\mathbf{x}) = 1 - \frac{\langle f(I), f(I'(\mathbf{x})) \rangle}{\|f(I)\| \cdot \|f(I'(\mathbf{x}))\|}$$

where $f(\cdot)$ denotes deep feature encoding, and $\langle \cdot, \cdot \rangle$ denotes the vector inner product. A FaceNet [1] model is trained and used as the deep feature extractor.

To prevent face shape and texture degeneration, we add a commonly-used loss on the regressed 3DMM coefficients for regularization:

$$L_{\text{coef}}(\mathbf{x}) = \omega_\alpha \|\alpha\|^2 + \omega_\beta \|\beta\|^2 + \omega_\gamma \|\delta\|^2$$

which enforces a prior distribution towards the mean face.

A flattening constraint is added to penalize the texture map variance:

$$L_{\text{tex}}(\mathbf{x}) = \sum_{c \in \{r, g, b\}} \text{var}(T_c, R(\mathbf{x}))$$

where R is a pre-defined skin region covering cheeks, nose, and forehead.

In summary, the loss function for R-Net is composed of two image-level losses, a perceptual loss, and two regularization losses.

5.1.2 Weakly-supervised Neural Aggregation for Multi-Image Reconstruction

To reconstruct a 3D face shape from multiple face images of a subject, we use a weakly-supervised neural aggregation method. Given an image set $\mathcal{I} := \{I^j | j = 1, \dots, M\}$, we use a network, C-Net, to predict a confidence vector $\mathbf{c} \in \mathbb{R}^{80}$ that measures the confidence of the identity-bearing shape coefficients $\alpha^j \in \mathbb{R}^{80}$ for each image j . The final aggregated

shape coefficient α_{aggr} is obtained via element-wise shape coefficient aggregation using the confidence scores:

$$\alpha_{\text{aggr}} = \left(\sum_j \mathbf{c}^j \odot \alpha^j \right) \oslash \left(\sum_j \mathbf{c}^j \right)$$

where \odot and \oslash denote the Hadamard product and division, respectively.

C-Net is trained in a label-free manner using image sets. We generate the reconstructed image set $\{I'^j\}$ of $\{I^j\}$ with $\{\hat{\mathbf{x}}^j\}$, where $\hat{\mathbf{x}}^j = (\alpha_{\text{aggr}}, \beta^j, \delta^j, p^j, \gamma^j)$. The training loss is defined as:

$$L(\{\hat{\mathbf{x}}^j\}) = \frac{1}{M} \sum_{j=1}^M L(\hat{\mathbf{x}}^j)$$

where $L(\cdot)$ is our hybrid-level loss function.

The error is backpropagated to α_{aggr} , further to \mathbf{c} , and C-Net weights since the aggregation process is differentiable. C-Net is trained to produce confidences that lead to an aggregated 3D face shape consistent with the image set.

The aggregation design and training scheme are inspired by set-based face recognition work [18]. We demonstrate that element-wise scores yield superior results and show how our network leverages face pose difference for better shape aggregation.

C-Net has a lightweight structure, reusing feature maps from R-Net for efficiency.

5.2 ResNet

As our classification model, we utilized ResNet-34, a deep convolutional neural network architecture. ResNet-34 is known for its ability to handle complex image classification tasks effectively.

In our case, we input the 80-dimensional shape coefficient vector α or 64-dimensional expression coefficient vector β into the ResNet-34 model for classification. The goal is to classify the input shape coefficient vector α or expression coefficient vector β into appropriate categories based on the task requirements.

For training the ResNet-34 model, we employed the cross-entropy loss function \mathcal{L}_{CE} . This loss function is commonly used in multi-class classification problems and helps to optimize the model’s parameters to improve classification accuracy. The cross-entropy loss is defined as:

$$\mathcal{L}_{\text{CE}}(p, q) = - \sum_i p_i \log(q_i)$$

where p represents the true class probability distribution, and q represents the predicted class probability distribution. Using ResNet-34 and the cross-entropy loss, our model can effectively learn to classify the input shape coefficient vectors and perform well on the given classification task.

6 Experiment Results

In this section, we present the results of our experiments using the KDEF and FEI face databases to evaluate the effectiveness of using alpha and beta coefficients for classification tasks. To measure the computational efficiency, the experiments were performed on a MacBook Air equipped with Apple’s M1 chip, which includes an 8-core GPU. Pytorch uses Metal Performance Shaders (MPS) for training acceleration.

6.1 Face Recognition (KDEF)

For this experiment, we used the KDEF dataset, which consists of 4900 pictures of human facial expressions from 70 individuals, each displaying 7 different emotional expressions viewed from 5 different angles.

We picked 10 different people’s pictures from the dataset, and divided into a training set containing 200 pictures and a validation set containing 150 pictures. For training the network, we experimented with two different input representations: original images and alpha coefficients (a 1×80 array) obtained using the following process. For each individual, we generated an alpha from each of the training 20 pictures available. We then selected 3 alphas out of the 20 in $\binom{20}{3} = 1140$ ways, resulting in 1140 sets of 3 alphas. Each set of 3 alphas was combined using C-Net to create one combined alpha. In validation, we also use the combined $\binom{15}{3} = 455$ alphas from originally 15 images for each individual.

The results of the classification by images showed an accuracy of 87.3%, while the classification by alpha achieved 100% accuracy. We conducted cross-validation to verify the results, and the accuracy remained consistent.

In addition, the average training time for each input is about 0.054s by using images and 0.005s by using alpha. This shows a significant improvement in training and classifying time.

6.2 Classification of Expressions (KDEF)

In this experiment, we aimed to classify different emotional expressions using the KDEF dataset, which consists of 4900 pictures of human facial expressions from 70 individuals, each displaying 7 different emotional expressions viewed from 5 different angles.

To perform the classification, we split all the photos into 7 categories, each representing one emotional expression. We created a training set containing 2975 pictures and a validation set containing 1925 pictures.

For the classification task, we used the beta coefficients (expression coefficients) as input for one set of experiments and the original images as input for another set of experiments.

After cross-validation, the results of the classification using beta coefficients showed an average accuracy of 83.5%, whereas the classification using original images achieved an accuracy of 70.6%. The significant improvement in accuracy when using beta coefficients demonstrates the effectiveness of shape-based representations for capturing the variations in different emotional expressions.

In addition, the training time using images ranges from 150.76 to 219.61 seconds per epoch. However, using β reduces the training time significantly to a range of 4.05 to 4.33 seconds per epoch.

6.3 Classification of Gender (FEI Face Database)

In this experiment, we used the FEI face database, which contains 2800 colorful face images of 200 individuals, evenly distributed between 100 males and 100 females. The images were taken in an upright frontal position with profile rotation of up to about 180 degrees.

We split the dataset into a training set with 50 male and 50 female images and a validation set with the remaining 50 male and 50 female images.

Using the original images for classification, the accuracy achieved was 79.8%. However, when using alpha coefficients for classification, the average accuracy significantly improved to 95.4% after cross-validation.

Training time using images ranges from 79.10 to 99.56 seconds per epoch. On the other hand, by utilizing α coefficients, the training time was reduced to a range of 38.18 to 44.56 seconds per epoch, resulting in a notable improvement in training time.

7 Analysis

The experimental results demonstrate that using alpha and beta coefficients as inputs for classification tasks yields superior accuracy with shorter training time compared to using the original images directly. This indicates that the shape information encoded in the alpha coefficients and expression information encoded in beta coefficients plays a crucial role in improving the classification performance.

7.1 Classification Results

Classification Task	Using Images	Using 3DMM Coefficients
Face Recognition (KDEF)	87.3%	100%
Classify Expression (KDEF)	70.6%	83.5%
Classify Gender (FEI)	79.8%	95.4%

Table 1: Classification Results Using Different Inputs

Table 1 shows the accuracy achieved for each classification task using different inputs. It can be observed that using alpha and beta coefficients significantly improves the accuracy in both tasks, outperforming the use of original images directly.

7.2 Training Time Comparison

Classification Task	Using Images	Using 3DMM Coefficients
Face Recognition	0.054s	0.005s
Classify Expression	0.062s	0.001s
Classify Gender	0.006s	0.003s

Table 2: Average Training Time (Each Input) Using Different Inputs

Table 2 shows that the proposed model utilizing 3DMM coefficients significantly reduces training time compared to using the original images. Across all three classification tasks (Face Recognition, Classify Expression, and Classify Gender), the training time using 3DMM coefficients is considerably faster than using images. On average, the training time is reduced by factors ranging from approximately 2 to 62 times. This time-saving advantage enables faster model development, deployment, and real-time classification applications. Additionally, the reduced complexity in the feature space provided by 3DMM coefficients enhances the overall time efficiency of the proposed model.

7.3 Expression Analysis

	AF	AN	DI	HA	NE	SA	SU
AF	75.26%	1.10%	3.87%	1.66%	2.40%	5.00%	10.70%
AN	4.24%	65.00%	13.09%	1.11%	8.29%	7.56%	0.73%
DI	3.49%	2.76%	86.75%	1.11%	0.18%	5.34%	0.37%
HA	0.74%	0.74%	1.29%	95.77%	0.37%	0.74%	0.37%
NE	0.18%	1.83%	0%	0%	93.22%	4.76%	0%
SA	3.12%	1.65%	4.58%	0.18%	9.71%	80.57%	0.18%
SU	12.19%	0.55%	0%	0.19%	0.74%	0.55%	85.78%

Table 3: The Confusion Matrix Using Proposed Method in Expression Classification

The abbreviations 'AF,' 'AN,' 'DI,' 'HA,' 'NE,' 'SA,' and 'SU' in table 3 correspond to the emotions afraid, angry, disgust, happy, neutral, sad, and surprise, respectively. Upon analyzing the confusion matrix, it is evident that some

expressions have lower accuracy compared to others. For example, the accuracy for the 'AN' (angry) expression is only 65.00%, which is relatively low compared to other emotions. Possible reasons for this lower accuracy could include the complexity and subtle variations in the facial expressions associated with anger, which might make it more challenging for the classification model to accurately identify.

7.4 Future Work

Overall, our experiments confirm the effectiveness of utilizing 3DMM coefficients for facial image classification tasks and highlight the potential of shape-based representations for face analysis and recognition.

To expand the scope of applicability for 3DMM models and parameters, it is important to conduct further investigation into integrating them into more intricate and demanding classification tasks. This future work aims to explore the potential benefits and challenges associated with integrating 3DMM models and parameters in such tasks.

8 Conclusion

Our novel approach for facial analysis using shape-based representations and weakly-supervised neural aggregation achieved remarkable results in various tasks. By employing 3DMM for facial shape representation, we demonstrated the effectiveness of alpha and beta coefficients, achieving 100% accuracy in individual classification, 95.4% accuracy in gender classification, and 83.5% in expression classification.

The integration of deep feature encoding and perception-level loss enhanced the robustness of our approach, making it resilient to occlusions and diverse appearance variations. Our method showcased versatility and efficacy for facial classification tasks, laying the groundwork for advancements in various domains.

In conclusion, our research highlights the potential of shape-based and expression-based representations and weakly-supervised neural aggregation for facial analysis. Our innovative techniques contribute to improved accuracy and open new avenues for real-world applications.

References

- [1] Florian Schroff, Dmitry Kalenichenko, and James Philbin. Facenet: A unified embedding for face recognition and clustering. In *Proceedings of the IEEE conference on computer vision and pattern recognition*, pages 815–823, 2015.
- [2] Kaiming He, Xiangyu Zhang, Shaoqing Ren, and Jian Sun. Deep residual learning for image recognition. In *Proceedings of the IEEE conference on computer vision and pattern recognition*, pages 770–778, 2016.
- [3] Yi Sun, Xiaogang Wang, and Xiaoou Tang. Deep learning face representation from predicting 10,000 classes. In *Proceedings of the IEEE conference on computer vision and pattern recognition*, pages 1891–1898, 2014.
- [4] Yaniv Taigman, Ming Yang, Marc’Aurelio Ranzato, and Lior Wolf. Deepface: Closing the gap to human-level performance in face verification. In *Proceedings of the IEEE conference on computer vision and pattern recognition*, pages 1701–1708, 2014.
- [5] SK Eng, H Ali, AY Cheah, and YF Chong. Facial expression recognition in jaffe and kdef datasets using histogram of oriented gradients and support vector machine. In *IOP Conference series: materials science and engineering*, volume 705, page 012031. IOP Publishing, 2019.
- [6] Carlos Eduardo Thomaz and Gilson Antonio Giraldi. A new ranking method for principal components analysis and its application to face image analysis. *Image and vision computing*, 28(6):902–913, 2010.
- [7] Ming-Hei Wong, Meixi Li, King-Man Tam, Hoi-Man Yuen, Chun-Ting Au, Kate Ching-Ching Chan, Albert Martin Li, and Lok-Ming Lui. A quasiconformal-based geometric model for craniofacial analysis and its application. *Axioms*, 12(4):393, 2023.
- [8] Volker Blanz and Thomas Vetter. Face recognition based on fitting a 3d morphable model. *IEEE Transactions on pattern analysis and machine intelligence*, 25(9):1063–1074, 2003.
- [9] Yu Deng, Jiaolong Yang, Sicheng Xu, Dong Chen, Yunde Jia, and Xin Tong. Accurate 3d face reconstruction with weakly-supervised learning: From single image to image set. In *Proceedings of the IEEE/CVF conference on computer vision and pattern recognition workshops*, pages 0–0, 2019.
- [10] Daniel Lundqvist, Anders Flykt, and Arne Öhman. Karolinska directed emotional faces. *PsycTESTS Dataset*, 91:630, 1998.
- [11] C.E. (Caru) Thomaz. Fei face database. Available online: <http://fei.edu.br/cet/facedatabase.html> (accessed on 15 May 2017), 2017.
- [12] Pascal Paysan, Reinhard Knothe, Brian Amberg, Sami Romdhani, and Thomas Vetter. A 3d face model for pose and illumination invariant face recognition. In *2009 sixth IEEE international conference on advanced video and signal based surveillance*, pages 296–301. Ieee, 2009.
- [13] Yudong Guo, Jianfei Cai, Boyi Jiang, Jianmin Zheng, et al. Cnn-based real-time dense face reconstruction with inverse-rendered photo-realistic face images. *IEEE transactions on pattern analysis and machine intelligence*, 41(6):1294–1307, 2018.
- [14] Ravi Ramamoorthi and Pat Hanrahan. An efficient representation for irradiance environment maps. In *Proceedings of the 28th annual conference on Computer graphics and interactive techniques*, pages 497–500, 2001.
- [15] Ravi Ramamoorthi and Pat Hanrahan. A signal-processing framework for inverse rendering. In *Proceedings of the 28th annual conference on Computer graphics and interactive techniques*, pages 117–128, 2001.
- [16] Michael J Jones and James M Rehg. Statistical color models with application to skin detection. *International journal of computer vision*, 46:81–96, 2002.
- [17] Adrian Bulat and Georgios Tzimiropoulos. How far are we from solving the 2d & 3d face alignment problem?(and a dataset of 230,000 3d facial landmarks). In *Proceedings of the IEEE international conference on computer vision*, pages 1021–1030, 2017.

- [18] Jiaolong Yang, Peiran Ren, Dongqing Zhang, Dong Chen, Fang Wen, Hongdong Li, and Gang Hua. Neural aggregation network for video face recognition. In *Proceedings of the IEEE conference on computer vision and pattern recognition*, pages 4362–4371, 2017.